



# Tiara[5]arenes: Synthesis, Solid-State Conformational Studies, Host–Guest Properties, and Application as Nonporous Adaptive Crystals

Weiwei Yang<sup>+</sup>, Kushal Samanta<sup>+</sup>, Xintong Wan<sup>+</sup>, Tushar Ulhas Thikekar, Yang Chao, Shunshun Li, Ke Du, Jun Xu, Yan Gao, Han Zuilhof,\* and Andrew C.-H. Sue\*

**Abstract:** Tiara[5]arenes (T[5]s), a new class of five-fold symmetric oligophenolic macrocycles that are not accessible from the addition of formaldehyde to phenol, were synthesized for the first time. These pillar[5]arene-derived structures display both unique conformational freedom, differing from that of pillararenes, with a rich blend of solid-state conformations and excellent host–guest interactions in solution. Finally we show how this novel macrocyclic scaffold can be functionalized in a variety of ways and used as functional crystalline materials to distinguish uniquely between benzene and cyclohexane.

## Introduction

More than half a century since Pederson's seminal discovery of synthetic host molecules,<sup>[1]</sup> the scope of macrocyclic chemistry is still expanding.<sup>[2]</sup> Apart from well-established classes such as cyclodextrins,<sup>[3]</sup> cucurbiturils<sup>[4]</sup> and crown ethers,<sup>[5]</sup> a large number of synthetic macrocycles has emerged. Many of these are derived de facto from one set of reactions: the condensation of phenols with aldehydes.<sup>[6]</sup> This gave rise (Figure 1) not only to bakelite,<sup>[7]</sup> but also to cyclotrimeratrylenes,<sup>[8]</sup> resorcinarenes,<sup>[9]</sup> calixarenes,<sup>[10]</sup> and in recent times to pillararenes<sup>[11]</sup> and other analogues.<sup>[12]</sup> Pillararenes, named after their characteristic cylindrical pillar-shaped cavities, have gained considerable popularity in the

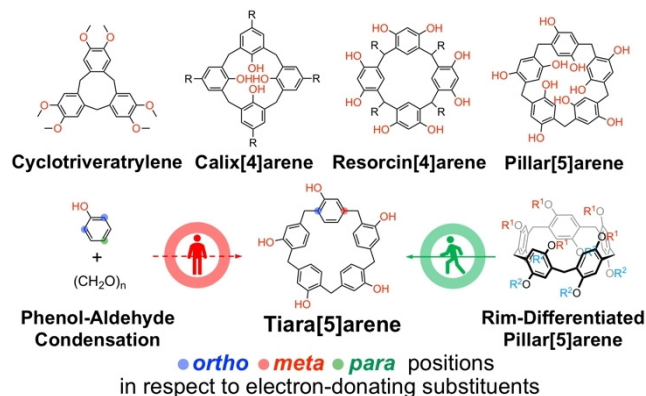


**Figure 1.** Tiara[5]arene, a *para*-bridged oligophenolic macrocycle, which is not attainable by condensing phenol and formaldehyde, can be synthesized by taking a detour through rim-differentiated pillar[5]arene.

past decade on account of their facile syntheses, versatility towards derivatization, and rich host–guest chemistry. The synthesis of the pentameric homologue, pillar[5]arene<sup>[13]</sup> (P[5]), is especially high-yielding, allowing the construction of a wide range of supramolecular architectures based on symmetric P[5]s with identical functionalities on both rims. Furthermore, recent developments from our group and others have opened up rim-specific functionalizations, leading to the so-called rim-differentiated<sup>[14–16]</sup> P[5]s (RD-P[5]s) with different top and bottom rims ( $R^1 \neq R^2$ ; Figure 1) to be prepared and further functionalized in a tailor-made fashion.

No *para*-bridged macrocycle arising from simply reacting phenol and formaldehyde is so far known, since one of the anchoring positions of the methylene bridges on the aromatic unit is not compatible with the well-known regioselectivity of the electrophilic substitution of phenol. Noting, for example, the extensive chemistry developed for calixarenes, which could be regarded as *meta*-bridged analogues, the conception of such unconventional macrocycles would open up as yet uncharted chemical space. Whereas the vast majority of current pillararene functionalizations are executed on the alkoxy moieties,<sup>[17]</sup> we reasoned that the specific removal of the O atoms on one side of RD-P[5]s to create a C–H functionalized rim would allow the construction of for example, C–C, C–N, and C–X bonds directly linked to the aromatic units, creating new opportunities for host–guest chemistry and novel scaffold construction approaches.

Herein we present the synthesis and solid-state structures of RD-P[5]-derived macrocycles composed of five phenolic units *para*-bridged covalently by methylenes, subsequently referred to as tiara[5]arenes (T[5]s) or tiararenes. Next, we

[\*] W. Yang,<sup>[†]</sup> Dr. K. Samanta,<sup>[†]</sup> X. Wan,<sup>[†]</sup> Dr. T. U. Thikekar, Y. Chao, S. Li, K. Du, Dr. J. Xu, Y. Gao, Prof. H. Zuilhof, Prof. A. C.-H. Sue  
Institute for Molecular Design and Synthesis, School of Pharmaceutical Science & Technology, Tianjin University  
92 Weijin Road, Nankai District, Tianjin 300072 (P. R. China)  
E-mail: andrew.sue@tju.edu.cn

Prof. H. Zuilhof

Laboratory of Organic Chemistry, Wageningen University  
Stippeneng 4, 6708 WE Wageningen (The Netherlands)  
and

Department of Chemical and Materials Engineering, Faculty of Engineering, King Abdulaziz University  
Jeddah (Saudi Arabia)  
E-mail: han.zuilhof@wur.nl

[†] These authors contributed equally to this work.

Supporting information and the ORCID identification number(s) for the author(s) of this article can be found under:  
<https://doi.org/10.1002/anie.201913055>.

© 2019 The Authors. Published by Wiley-VCH Verlag GmbH & Co. KGaA. This is an open access article under the terms of the Creative Commons Attribution Non-Commercial License, which permits use, distribution and reproduction in any medium, provided the original work is properly cited and is not used for commercial purposes.

discuss their host–guest chemistry, derivatization strategies, and remarkable potential as nonporous adaptive crystals (NACs),<sup>[18]</sup> especially the ability to distinguish between rather similar guests, such as benzene and cyclohexane.

## Results and Discussion

The key step in the synthesis of tiara[5]arenes is the initial formation of the RD-P[5] precursor. Instead of a heads-or-tails statistical cyclization characterized by very low yields, our synthesis started with a monomer that aligns in a head-to-tail manner, resulting in a highly selective synthesis of RD-P[5]s, that is, 55 % selectivity among all four P[5] constitutional isomers and 20 % yields of isolated product.<sup>[14]</sup> In the beginning we set out to improve the yield of the RD-P[5] synthesis, widening a bottleneck in our synthesis. One major limitation to be overcome in the oligocyclization is the retro-Friedel–Crafts reaction; after formation of the aryl–CH<sub>2</sub>–aryl moiety, the reaction can reverse.<sup>[19]</sup> The result is the generation of the other three undesired P[5] isomers, rather than an exclusive synthesis of RD-P[5] that would have occurred had this retro Friedel–Crafts reaction not occurred (see the Supporting Information). Reduction of the water content by using CaH<sub>2</sub>-dried 1,2-dichloroethane as solvent suppressed this retro effect and routinely increased the yield of (OBn)<sub>5</sub>-RD-P[5] from 20<sup>[15]</sup> to 25 %, leading to a gram-scale production in one step (Scheme 1).

Subsequently, the benzyl groups were removed using ammonium formate as a hydrogen source in the presence of Pd/C, and the deprotected penta-OH intermediate was converted directly to the air-stable (OTf)<sub>5</sub>-RD-P[5] in 87 % yield in two steps. This penta-triflate was hydrodeoxygenated by reduction (H<sub>2</sub> over Pd/C) under slightly basic conditions to convert all five OTf groups into H atoms, providing access to the permethylated tiara[5]arene (T[5]-(OMe)<sub>5</sub>) in 96 % yield. Near-quantitative *O*-demethylation with excess of BBr<sub>3</sub> finally yields the parent tiara[5]arene (T[5]), a new macrocyclic scaffold consisting of phenol units linked by methylene bridges anchored on the *ortho*- and *meta*-positions with respect to the OH groups. The total yield over five steps is 20 %, allowing us to synthesize 410 mg of T[5] from per gram of the (OBn)<sub>5</sub>-RD-P[5] precursor produced.

Tiara[5]arene and T[5]-(OMe)<sub>5</sub> show in solution (for example, observed in the NMR spectra) an averaged C<sub>5</sub> symmetry on account of their high conformational freedom similar to [1<sub>5</sub>]paracyclophane.<sup>[20,21]</sup> The structural flexibility is also evidenced by the rich polymorphism of T[5]-(OMe)<sub>5</sub> displayed in the solid state, a selection of which are displayed

in Figure 2 (see the Supporting Information for more polymorphs). A solvent-free T[5]-(OMe)<sub>5</sub> structure<sup>[22]</sup> (space group  $P\bar{1}$ , triclinic) obtained on crystallization by vapor diffusion of CH<sub>3</sub>OH into CHCl<sub>3</sub> solution, features a C<sub>1</sub> conformation (Figure 2a), with the cavity-forming rings alternatingly up and down. With the odd number of aryl

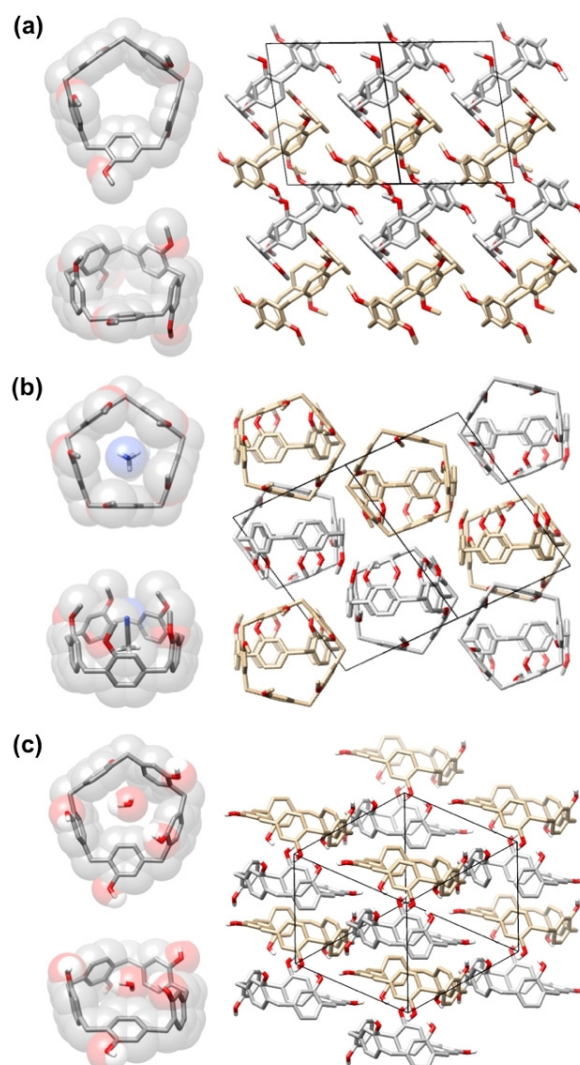
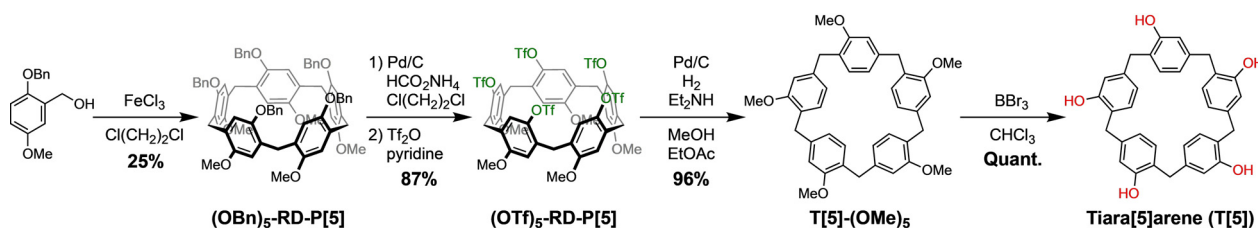


**Figure 2.** X-ray crystal structures of a) T[5]-(OMe)<sub>5</sub>, b) CH<sub>3</sub>CN·T[5]-(OMe)<sub>5</sub>, and c) H<sub>2</sub>O·T[5]-(OMe)<sub>5</sub>, showing assorted solid-state conformations of the tiara[5]arene scaffold. Packing modes in (a), (b), and (c) are viewed from [1 $\bar{1}$ 0], [110], and [111] directions, respectively. Most hydrogen atoms and solvent molecules are omitted for clarity. C silver/gold for different enantiomeric conformers, O red, N blue, H white.



**Scheme 1.** The metamorphosis of rim-differentiated pillar[5]arenes (RD-P[5]s) into tiara[5]arenes (T[5]s).

rings, this alternation leaves one remaining ring to be rotated nearly 90° with respect to the other four rings. While this rotation has also been observed for [1<sub>5</sub>]paracyclophane and for the leaning pillar[6]arene,<sup>[23]</sup> this rotational distortion is not intrinsic to these C–H functionalized *para*-bridged macrocycles.

C<sub>1</sub>-symmetrical conformations can also be found in single crystals obtained under different conditions, such as vapor diffusion of CH<sub>3</sub>OH into *trans*-1,2-dichloroethene or EtOAc solutions, although in both cases the T[5]-(OMe)<sub>5</sub> conformations deviate from the one shown in Figure 2a: from 1,2-dichloroethene, apart from 2 up, 2 down, 1 flat macrocycles, a 3 up, 1 down, 1 flat conformation can also be obtained. In the crystal structure obtained in EtOAc, another 3 up, 2 down geometry can be also observed. In other words, T[5]s by themselves do not typically display pillar-like structures.

The inclusion of a CH<sub>3</sub>CN solvent molecule changes (Figure 2b) this picture. Similar to many P[5] derivatives, in the CH<sub>3</sub>CN⊂T[5]-(Me)<sub>5</sub> crystal structure<sup>[24]</sup> (space group *P* $\bar{1}$ , triclinic) all five aromatic units are now aligned almost perpendicularly to the pentagonal plane formed by the carbon atoms on the methylene bridges, and result in a more or less five-fold symmetric tiara-like cavity of diameter ca. 8 Å. A CH<sub>3</sub>CN molecule is located inside. Both C–H⋯π (distances 2.95, 3.29, and 3.41 Å) and C–H⋯N interactions (distances 2.74, 2.77, 2.98, 3.04, and 3.14 Å) can be found between the T[5]-(OMe)<sub>5</sub> macrocycle and the CH<sub>3</sub>CN guest molecule. Interestingly, the CH<sub>3</sub>CN is oriented in only one of the two possible directions, indicating a strong orientational preference, presumably as a result of dipole stabilization. This complexation geometry is borne out by wB97XD/6–311 + G(d,p) calculations which confirm a preference of 6.2 kcal mol<sup>-1</sup> for the experimentally observed orientation of the CH<sub>3</sub>CN molecule in the cavity (see detailed computed structures in the Supporting Information).

The parent T[5] macrocycle can also be crystallized<sup>[25]</sup> in the space group *P* $\bar{1}$  (triclinic) by slow cooling in PhMe (Figure 2c). A distorted conformation, with one flat and four more vertical phenolic units relative to the pentagonal scaffold, can be found in the structure, even although the orientations and dihedral angles involving the aromatic rings differ from those of the T[5]-(OMe)<sub>5</sub> polymorphs (Figure 2a,b and the Supporting Information). Multiple hydrogen bonds are present between adjacent macrocycles, via interactions between the phenol groups (O–H⋯O distances 1.89, 1.69, and 2.00 Å). Apart from PhMe solvent molecules in the interstices between the T[5] macrocycles, an H<sub>2</sub>O molecule (most likely absorbed from the surroundings) is also found in the cavity. An H-atom of this water is hydrogen-bonded with a phenolic O-atom of the adjacent T[5] (O–H⋯OH<sub>2</sub>, distance 1.92 Å).

The observation of these solvent-inclusion complexes prompted us to study the host–guest chemistry of tiara[5]arene. Cationic guests, such as methyl viologen (MV<sup>2+</sup>), methylpyridinium (Py<sup>+</sup>), and a linear alkyl chain 1,6-dicyanohexane guest were screened (Figure 3 and the Supporting Information) by NMR titration experiments. In a 1:1 mixture of the T[5] host (5 mM in MeOD-*d*<sub>4</sub>) and 5 mM Py-Cl, all <sup>1</sup>H NMR signals of the cationic guest showed a pronounced

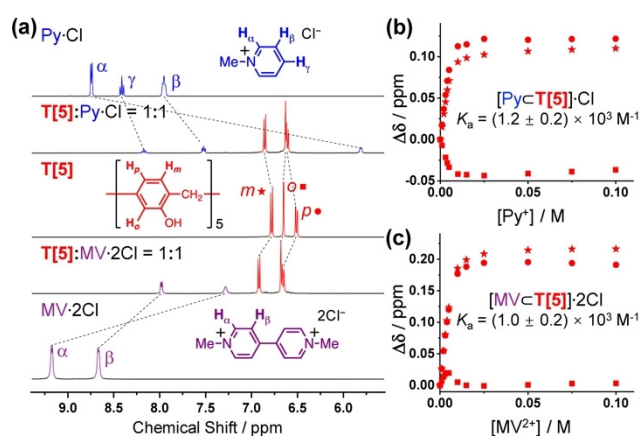


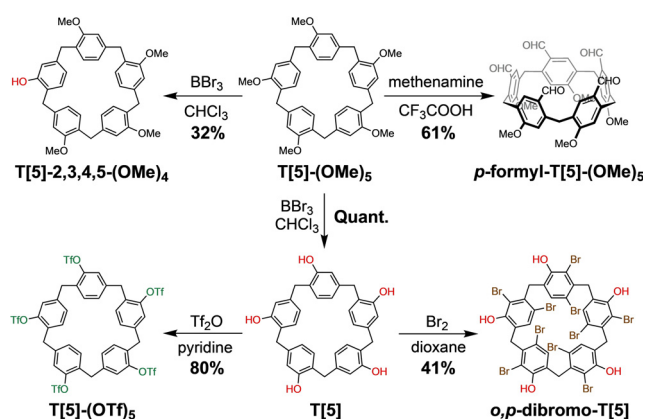
**Figure 3.** Host–guest interactions between tiara[5]arene and cationic species. a) Partial <sup>1</sup>H NMR spectra (400 MHz, MeOD-*d*<sub>4</sub>, 298 K) of T[5], chloride salts of methylpyridinium and methyl viologen, and their 1:1 mixtures at 5 mM concentrations. b), c) The association constants of b) [Py⊂T[5]·Cl and c) [MV⊂T[5]·2Cl 1:1 complexes in MeOD-*d*<sub>4</sub> are determined by NMR titration method.

upfield shift ( $\Delta\delta$  of H <sub>$\alpha$</sub> , H <sub>$\beta$</sub>  and H <sub>$\gamma$</sub>  = 3.2, 0.4, and 0.6 ppm, respectively), as a result of the shielding effect commensurate with host–guest complexation. Similar upfield shifts ( $\Delta\delta$  of H <sub>$\alpha$</sub>  and H <sub>$\beta$</sub>  = 2.0 and 0.7 ppm, respectively) were observed for an analogous experiment with MV<sup>2+</sup>. Owing to the absence of one set of electron-donating OH group in the aromatic unit, the electron density of the T[5] cavity is relatively poor compared to those of regular P[5]s. Furthermore, the high conformational freedom of the T[5] scaffold, evidenced by its very simple <sup>1</sup>H NMR spectrum, would also lead to a comparatively increased entropy loss upon guest binding. Nonetheless, the T[5] host still exhibits good binding affinities to these cationic guests in CH<sub>3</sub>OH, with association constants  $K_a$  of  $(1.2 \pm 0.2) \times 10^3$  and  $(1.0 \pm 0.2) \times 10^3$  M<sup>-1</sup> for Py-Cl and MV·2Cl in a 1:1 binding mode, respectively. In contrast, 1,6-dicyanohexane, which is commonly used in P[5] host–guest systems,<sup>[26]</sup> shows a binding constant value of typically 1–2 orders of magnitude lower (see the Supporting Information), demonstrating the significant difference in binding preference towards guests between homologous T[5] and P[5] macrocycles.

Subsequent functionalization on either T[5] or T[5]-(OMe)<sub>5</sub> could be achieved (Scheme 2) in a variety of ways. First, for T[5] the OH groups can be functionalized, in analogy to our previous work<sup>[15]</sup> on rim-differentiated P[5]s, by alkylation, esterification, or Suzuki–Miyaura coupling and SuFEx reactions, after being converted to triflates and sulfonyl fluorides, respectively. The corresponding penta-triflate T[5]-(OTf)<sub>5</sub>, for example, was synthesized in 80% yield (see the Supporting Information).

Given the presence of OH or OMe activating groups, tiara[5]arenes can be easily functionalized by regioselective electrophilic substitutions. Under Duff formylation conditions, T[5]-(OMe)<sub>5</sub> was transformed successfully into penta-*para*-substituted *p*-formyl-T[5]-(OMe)<sub>5</sub> in 61% yield.<sup>[27]</sup> Various bromination conditions were also tested, with the relative mild water–bromine system providing the highest yield





**Scheme 2.** Versatile derivatizations of the tiara[5]arene scaffold at the *ortho*, *para*, and phenolic positions.

(41%) of an isomerically pure decabromide derivative *o,p*-dibromo-T[5]. Interestingly, it was found that bromination is a fast reaction, that is, completed in minutes, and not only on the five *para*- but also at all five *ortho*-positions. Mass spectrometry analysis shows good agreement in isotopic distributions with the decabromide product (see the Supporting Information).

Apart from highly symmetric penta- and deca-functionalizations, we have also focused on strategies to address a single aromatic ring in T[5]s selectively. Such mono-functionalized<sup>[28]</sup> macrocycles are highly desirable building blocks for developing various supramolecular architectures and functional systems. Whereas cleavage of the ether bonds on perfunctionalized pillar[5]arenes results in numerous isomeric products,<sup>[29]</sup> partial demethylation of penta-methylate T[5]-(OMe)<sub>5</sub> by 1 equiv of BBr<sub>3</sub> led to a much less complicated reaction product mixture.<sup>[30]</sup> As a result, mono-deprotected T[5]-2,3,4,5-(OMe)<sub>4</sub> could be isolated in a reasonable yield of 32% by column chromatography.<sup>[31]</sup> We believe the field of mono-functionalized tiaraarenes may be open to a wide range of applications not easily available to other macrocycles.

Finally, attention was given to the possibility of using tiaraarene-based materials for separation purposes. Many oligophenol macrocycles, especially calix[4]arenes, have been found<sup>[32]</sup> to exhibit single-crystal-to-single-crystal transformations in the solid state upon guest inclusion and/or gas absorption. More recently, pillararene-based crystalline organic materials have also been shown<sup>[33]</sup> to be effective for the separation of linear/branched

alkanes, xylene isomers, styrene/ethylbenzene, toluene/methyl-cyclohexane, and dihalobenzene isomers. Analogously, the triangular biphen[3]arene macrocycle was used<sup>[12g]</sup> to discriminate *cis*- over *trans*-dichloroethene during preferential solid-vapor uptake, and dual-selective fractionations of chlorobenzene/chlorocyclohexane by two polymorphs of geminiarene featuring different conformations were also reported.<sup>[12h]</sup> These findings all intrigued us to investigate the solid-state host-guest chemistry of tiara[5]arene-based crystalline materials.

Permethyated T[5]-(OMe)<sub>5</sub> was chosen for the ease of straightforward crystallization by vapor diffusion of CH<sub>3</sub>OH into a CH<sub>3</sub>CN solution. The resulting CH<sub>3</sub>CN⊂T[5]-(OMe)<sub>5</sub> crystals were then subjected to vacuum at elevated temperature to remove solvent guest molecules from the cavity. Powder X-ray diffraction (PXRD) characterization of T[5]-(OMe)<sub>5</sub> materials before and after activation confirms (Figure 4a,b) their crystalline nature. Preliminary solid-vapor sorption experiments were carried out to test the uptake capacity and selectivity of the activated T[5]-(OMe)<sub>5</sub> crystalline material. It was found that T[5]-(OMe)<sub>5</sub> strongly favors aromatic benzene derivatives over their aliphatic counterparts.

The separation of benzene and cyclohexane is an important industrial process particularly in view of their interdependence, for example, cyclohexane is obtained from the catalytic hydrogenation of benzene.<sup>[34]</sup> The minute 0.7 K difference between the boiling points of benzene (353.2 K) and cyclohexane (353.9 K) imposes a great challenge for various distillation and purification processes. To test its capability for benzene/cyclohexane fractionation, time-dependent sorption experiments were conducted on activated T[5]-(OMe)<sub>5</sub> samples over a mixture of benzene/cyclohexane (50:50 v/v). <sup>1</sup>H NMR analysis showed that benzene uptake increased rapidly within the first hour and eventually reached

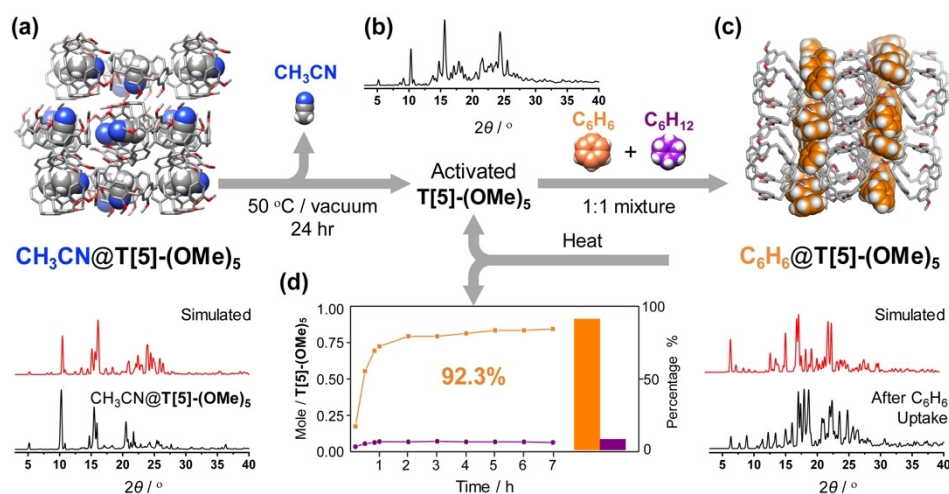


**Figure 4.** Outline of the benzene/cyclohexane fractionation process involving tiara[5]arene-based non-porous adaptive crystals. a) First, crystals of T[5]-(OMe)<sub>5</sub> obtained from CH<sub>3</sub>CN were subjected to heat/vacuum for solvent removal. b) The activated T[5]-(OMe)<sub>5</sub> crystalline material was exposed to a 1:1 benzene/cyclohexane mixture vapor (50:50 v/v) under ambient conditions. c) Subsequent PXRD and X-ray crystallography analyses confirmed the phase change of T[5]-(OMe)<sub>5</sub> after vapor adsorption, while d) <sup>1</sup>H-NMR time-dependent vapor-solid sorption plot and gas chromatography analysis revealed the preferential uptake of benzene over cyclohexane.

about 0.8 equiv per tiara[5]arene ring after saturation, whereas relatively small amount of cyclohexane is also present in the crystals. Gas chromatography confirmed (Figure 4d) that benzene accounts for 92.3% of total guest uptake in T[5]-(OMe)<sub>5</sub>. Upon heating, the benzene molecules adsorbed are released and the T[5]-(OMe)<sub>5</sub> can be reactivated for repeated fractionation cycles (see the Supporting Information).

The PXRD patterns of activated T[5]-(OMe)<sub>5</sub> before and after benzene uptake are significantly different, indicating (Figure 4c, bottom) the formation of a new crystalline phase upon the adsorption of benzene. To elucidate the structural transformations of the T[5]-(OMe)<sub>5</sub> crystalline materials resulting from the adsorption process, T[5]-(OMe)<sub>5</sub> was crystallized from benzene after slow evaporation and analyzed by X-ray crystallography. The C<sub>6</sub>H<sub>6</sub>@T[5]-(OMe)<sub>5</sub> superstructure<sup>[35]</sup> features (Figure 4c, top) a distorted conformer which stacks along the crystallographic *c*-axis. Instead of forming inclusion complexes with T[5]-(OMe)<sub>5</sub>, the benzene molecules are found in the interstices between stacks of macrocycles. A simulated PXRD pattern of the C<sub>6</sub>H<sub>6</sub>@T[5]-(OMe)<sub>5</sub> crystal structure, bears resemblance to the experimental PXRD pattern of T[5]-(OMe)<sub>5</sub> after benzene exposure, indicating that the permethylated tiara[5]arene selectively recrystallized with benzene upon solid-vapor contact.

## Conclusion

In summary, we have synthesized an oligophenol-based macrocycle, tiara[5]arene, which is not obtainable by the direct, century-old condensation of phenol with formaldehyde. The synthesis detour took advantage of the efficient formation of rim-differentiated pillar[5]arenes, followed by the selective hydrodeoxygenation of one rim. X-ray crystallography studies revealed multifaceted conformations of tiara[5]arenes in the solid state. We demonstrated a range of functionalization routes specific for tiara[5]arenes, further expanding this class of compounds. In addition to the ability of binding cationic pyridinium and bipyridinium guests, tiara[5]arene-based crystalline materials showed highly selective fractionations of aromatic/aliphatic compounds during solid-vapor adsorption. We expect that these new macrocycles will find widespread applications in supramolecular chemistry, both in solution and in the solid state, and will serve as unique five-fold symmetric building blocks for constructing complex architectures.<sup>[36]</sup>

## Acknowledgements

This work was supported by the 973 National Basic Research Program of China (2015CB856500), National Science Foundation of China (H.Z., 21871208), Tianjin City Thousand Talents Program (H.Z. and A.C.-H.S.), Chinese National Thousand Talents Young Investigator Program (A.C.-H.S.), SAFEA foreign young talent program (K.S.), Wageningen University, and Tianjin University. We thank Prof. Xiangyang Zhang and all staff of Instrumental Analysis Center, School of Pharmaceutical Science and Technology, Tianjin University

for assistance in various characterizations, and Jia-Rui Wu, Prof. Ying-Wei Yang, Kaidi Xu, and Prof. Chunju Li for their help with the NACs experiments.

## Conflict of interest

The authors declare no conflict of interest.

**Keywords:** five-fold symmetry · host-guest chemistry · nonporous adaptive crystals · polymorphism · tiara[5]arene

**How to cite:** *Angew. Chem. Int. Ed.* **2020**, *59*, 3994–3999  
*Angew. Chem.* **2020**, *132*, 4023–4028

- [1] a) C. J. Pedersen, *J. Am. Chem. Soc.* **1967**, *89*, 2495–2496; b) C. J. Pedersen, *J. Am. Chem. Soc.* **1967**, *89*, 7017–7036.
- [2] J. W. Steed, J. L. Atwood, *Supramolecular Chemistry*, Wiley, Chichester, **2013**.
- [3] a) A. Villiers, *C. R. Hebd. Seances Acad. Sci.* **1891**, *112*, 536–538; b) V. T. D'Souza, K. B. Lipkowitz, *Chem. Rev.* **1998**, *98*, 1741–1742; c) G. Crini, *Chem. Rev.* **2014**, *114*, 10940–10975.
- [4] a) R. Behrend, E. Meyer, F. Rusche, *Justus Liebigs Ann. Chem.* **1905**, *339*, 1–37; b) W. A. Freeman, W. L. Mock, N. Y. Shih, *J. Am. Chem. Soc.* **1981**, *103*, 7367–7368; c) J. Kim, I.-S. Jung, S.-Y. Kim, E. Lee, J.-K. Kang, S. Sakamoto, K. Yamaguchi, K. Kim, *J. Am. Chem. Soc.* **2000**, *122*, 540–541.
- [5] a) M. Hiraoka, *Crown Ethers and Analogous Compounds*, Elsevier, Amsterdam, **2016**; b) C. J. Pedersen, *Science* **1988**, *241*, 536–540.
- [6] A. Baeyer, *Ber. Dtsch. Chem. Ges.* **1872**, *5*, 280–282.
- [7] a) L. H. Baekeland, US Patent 942 699, **1907**; b) D. Crespy, M. Bozonnet, M. Meier, *Angew. Chem. Int. Ed.* **2008**, *47*, 3322–3328; *Angew. Chem.* **2008**, *120*, 3368–3374.
- [8] M. J. Hardie, *Chem. Soc. Rev.* **2010**, *39*, 516–527.
- [9] a) P. Timmerman, W. Verboom, D. N. Reinhoudt, *Tetrahedron* **1996**, *52*, 2663–2704; b) S. M. Biro, J. Rebek, Jr., *Chem. Soc. Rev.* **2007**, *36*, 93–104; c) L. Pirondini, E. Dalcanale, *Chem. Soc. Rev.* **2007**, *36*, 695–706.
- [10] a) V. Böhmer, *Angew. Chem. Int. Ed. Engl.* **1995**, *34*, 713–745; *Angew. Chem.* **1995**, *107*, 785–818; b) C. D. Gutsche, *Calixarenes Revisited*, Royal Society of Chemistry, Cambridge **1998**; c) C. D. Gutsche, *Calixarenes, An Introduction*, Royal Society of Chemistry, Cambridge, **2008**.
- [11] a) T. Ogoshi, T.-a. Yamagishi, Y. Nakamoto, *Chem. Rev.* **2016**, *116*, 7937–8002; b) T. Ogoshi, *Pillararenes*, Royal Society of Chemistry, Cambridge, **2016**.
- [12] a) S. T. Schneebeli, C. Cheng, K. J. Hartlieb, N. L. Strutt, A. A. Sarjeant, C. L. Stern, J. F. Stoddart, *Chem. Eur. J.* **2013**, *19*, 3860–3868; b) T. Boinski, A. Cieszkowski, B. Rosa, A. Szumna, *J. Org. Chem.* **2015**, *80*, 3488–3495; c) H. Chen, J. Fan, X. Hu, J. Ma, S. Wang, J. Li, Y. Yu, X. Jia, C. Li, *Chem. Sci.* **2015**, *6*, 197–202; d) G.-W. Zhang, P.-F. Li, Z. -Meng, H.-X. Wang, Yi. Han, C.-F. Chen, *Angew. Chem. Int. Ed.* **2016**, *55*, 5304–5308; *Angew. Chem.* **2016**, *128*, 5390–5394; e) L. Dai, Z.-J. Ding, L. Cui, J. Li, X. Jia, C. Li, *Chem. Commun.* **2017**, *53*, 12096–12099; f) B. Li, B. Wang, X. Huang, L. Dai, L. Cui, J. Li, X. Jia, C. Li, *Angew. Chem. Int. Ed.* **2019**, *58*, 3885–3889; *Angew. Chem.* **2019**, *131*, 3925–3929; g) Y. Wang, K. Xu, B. Li, L. Cui, J. Li, X. Jia, C. Li, *Angew. Chem. Int. Ed.* **2019**, *58*, 10281–10284; *Angew. Chem.* **2019**, *131*, 10387–10390; h) J. Wu, Y. Yang, *J. Am. Chem. Soc.* **2019**, *141*, 12280–12287.
- [13] a) T. Ogoshi, S. Kanai, S. Fujinami, T.-a. Yamagishi, Y. Nakamoto, *J. Am. Chem. Soc.* **2008**, *130*, 5022–5023; b) T. Ogoshi, T.

- Aoki, K. Kitajima, S. Fujinami, T.-a. Yamagishi, Y. Nakamoto, *J. Org. Chem.* **2011**, *76*, 328–331.
- [14] M. Guo, X. Wang, C. Zhan, P. Demay-Drouhard, W. Li, K. Du, M. A. Olson, H. Zuilhof, A. C.-H. Sue, *J. Am. Chem. Soc.* **2018**, *140*, 74–77.
- [15] P. Demay-Drouhard, K. Du, K. Samanta, X. Wan, W. Yang, R. Srinivasan, A. C.-H. Sue, H. Zuilhof, *Org. Lett.* **2019**, *21*, 3976–3980.
- [16] a) Y. Kou, H. Tao, D. Cao, Z. Fu, D. Schollmeyer, H. Meier, *Eur. J. Org. Chem.* **2010**, 6464–6470; b) Z. Zhang, Y. Luo, B. Xia, C. Han, Y. Yu, X. Chen, F. Huang, *Chem. Commun.* **2011**, *47*, 2417–2419; c) T. F. Al-Azemi, M. Vinodh, F. H. Alipour, A. A. Mohamod, *J. Org. Chem.* **2017**, *82*, 10945–10952; d) J. Ding, J. Chen, W. Mao, J. Huang, D. Ma, *Org. Biomol. Chem.* **2017**, *15*, 7894–7897.
- [17] N. L. Strutt, H. Zhang, S. T. Schneebeli, J. F. Stoddart, *Acc. Chem. Res.* **2014**, *47*, 2631–2642.
- [18] K. Jie, Y. Zhou, E. Li, F. Huang, *Acc. Chem. Res.* **2018**, *51*, 2064–2072.
- [19] M. Holler, N. Allenbach, J. Sonet, J.-F. Nierengarten, *Chem. Commun.* **2012**, *48*, 2576–2578.
- [20] a) G. W. Gribble, C. F. Nutaitis, *Tetrahedron Lett.* **1985**, *26*, 6023–6026; b) P. Liu, Q. Li, H. Zeng, B. Shi, J. Liu, F. Huang, *Org. Chem. Front.* **2019**, *6*, 309–312.
- [21] The rotational freedom of pillar[5]arenes has been investigated in detail, both experimentally and theoretically; see: a) T. Ogoshi, K. Kitajima, T. Aoki, S. Fujinami, T.-a. Yamagishi, Y. Nakamoto, *J. Org. Chem.* **2010**, *75*, 3268–3273; b) N. L. Strutt, S. T. Schneebeli, J. F. Stoddart, *Supramol. Chem.* **2013**, *25*, 596–608; c) X. Wang, R.-x. Chen, A. C.-H. Sue, H. Zuilhof, A. J. A. Aquino, H. Lischka, *Comput. Theor. Chem.* **2019**, *1161*, 1–9.
- [22] Crystallographic data for T[5]-(OMe)<sub>5</sub>: C<sub>40</sub>H<sub>40</sub>O<sub>5</sub>; colorless block, 0.2 × 0.2 × 0.2 mm<sup>3</sup>; triclinic, space group P $\bar{1}$ ;  $a = 11.30470(10)$ ,  $b = 12.60500(10)$ ;  $c = 12.78350(10)$  Å;  $\alpha = 76.1580(10)$ ,  $\beta = 88.8410(10)$ ,  $\gamma = 66.9490(10)^\circ$ ;  $V = 1621.97(3)$  Å<sup>3</sup>;  $Z = 2$ ;  $\rho_{\text{calc}} = 1.230$  g cm<sup>-3</sup>;  $2\theta_{\text{max}} = 149.378$ ;  $T = 160(10)$  K; 45791 reflections collected, 6363 independent, 411 parameters;  $\mu = 0.634$  mm<sup>-1</sup>;  $RI = 0.0513$  [ $I > 2\sigma(I)$ ],  $wR2 = 0.1472$  (all data).<sup>[37]</sup>
- [23] J.-R. Wu, A. U. Mu, B. Li, C.-Y. Wang, L. Fang, Y.-W. Yang, *Angew. Chem. Int. Ed.* **2018**, *57*, 9853–9858; *Angew. Chem.* **2018**, *130*, 10001–10006.
- [24] Crystallographic data for CH<sub>3</sub>CNCT[5]-(OMe)<sub>5</sub>: C<sub>42</sub>H<sub>43</sub>NO<sub>5</sub>; colorless block, 0.2 × 0.2 × 0.2 mm<sup>3</sup>; triclinic, space group P $\bar{1}$ ;  $a = 12.0935(2)$ ,  $b = 17.8479(3)$ ;  $c = 17.9763(2)$  Å;  $\alpha = 95.1170(10)$ ,  $\beta = 106.5750(10)$ ,  $\gamma = 105.9900(10)^\circ$ ;  $V = 3515.19(9)$  Å<sup>3</sup>;  $Z = 4$ ;  $\rho_{\text{calc}} = 1.213$  g cm<sup>-3</sup>;  $2\theta_{\text{max}} = 149.272$ ;  $T = 159.99(10)$  K; 34158 reflections collected, 12350 independent, 1069 parameters;  $\mu = 0.626$  mm<sup>-1</sup>;  $RI = 0.0701$  [ $I > 2\sigma(I)$ ],  $wR2 = 0.16$  (all data).<sup>[37]</sup>
- [25] Crystallographic data for H<sub>2</sub>OCT[5]: C<sub>42</sub>H<sub>40</sub>O<sub>6</sub>; yellow block, 0.2 × 0.2 × 0.2 mm<sup>3</sup>; triclinic, space group P $\bar{1}$ ;  $a = 10.1845(2)$ ,  $b = 12.1980(2)$ ;  $c = 15.5764(2)$  Å;  $\alpha = 98.7530(10)$ ,  $\beta = 102.834(2)$ ,  $\gamma = 107.544(2)^\circ$ ;  $V = 1748.27(6)$  Å<sup>3</sup>;  $Z = 2$ ;  $\rho_{\text{calc}} = 1.217$  g cm<sup>-3</sup>;  $2\theta_{\text{max}} = 149.204$ ;  $T = 310.60(10)$  K; 33007 reflections collected, 6919 independent, 604 parameters;  $\mu = 0.644$  mm<sup>-1</sup>;  $RI = 0.0532$  [ $I > 2\sigma(I)$ ],  $wR2 = 0.1600$  (all data).<sup>[37]</sup>
- [26] a) X. Shu, S. Chen, J. Li, Z. Chen, L. Weng, X. Jia, C. Li, *Chem. Commun.* **2012**, *48*, 2967–2969; b) Y. Wang, G. Ping, C. Li, *Chem. Commun.* **2016**, *52*, 9858–9872.
- [27] The formylation turned out to be rather specific in relation to reaction conditions, as under for example, Vilsmeier-Haak (POCl<sub>3</sub>/DMF) or Rieche formylation (Cl<sub>2</sub>CHOCH<sub>3</sub>/TiCl<sub>4</sub>), neither *p*- nor *o*-formyl-functionalized tiara[5]arenes could be obtained.
- [28] R. Lavendomme, A. Leroy, M. Luhmer, I. Jabin, *J. Org. Chem.* **2014**, *79*, 6563–6570.
- [29] a) T. Ogoshi, K. Demachi, K. Kitajima, T.-a. Yamagishi, *Chem. Commun.* **2011**, *47*, 7164–7166; b) N. L. Strutt, R. S. Forgan, J. M. Spruell, Y. Y. Botros, J. F. Stoddart, *J. Am. Chem. Soc.* **2011**, *133*, 5668–5671; c) Y. Chen, M. He, B. Li, L. Wang, H. Meier, D. Cao, *RSC Adv.* **2013**, *3*, 21405–21408; d) T. F. Al-Azemi, A. A. Mohamod, M. Vinodha, F. H. Alipoura, *Org. Chem. Front.* **2018**, *5*, 10–18.
- [30] Partial demethylation of T[5]-(OMe)<sub>5</sub> results in six different partially deprotected products in total.
- [31] The side product mixtures, containing partially-deprotected T[5]-(OMe)<sub>5</sub>, were collected and recycled for complete demethylation to T[5] in 57% yield (see the Supporting Information).
- [32] a) J. L. Atwood, L. J. Barbour, A. Jerga, *Science* **2002**, *296*, 2367–2369; b) J. L. Atwood, L. J. Barbour, A. Jerga, B. L. Schottel, *Science* **2002**, *298*, 1000–1002; c) J. L. Atwood, L. J. Barbour, A. Jerga, *Angew. Chem. Int. Ed.* **2004**, *43*, 2948–2950; *Angew. Chem.* **2004**, *116*, 3008–3010; for a more recent comprehensive review, see d) Y. Zhou, K. Jie, R. Zhao, F. Huang, *Adv. Mater.* **2019**, 1904824.
- [33] a) T. Ogoshi, R. Sueto, K. Yoshikoshi, Y. Sakata, S. Akine, T.-a. Yamagishi, *Angew. Chem. Int. Ed.* **2015**, *54*, 9849–9852; *Angew. Chem.* **2015**, *127*, 9987–9990; b) K. Jie, M. Liu, Y. Zhou, M. A. Little, S. Bonakala, S. Y. Chong, A. Stephenson, L. Chen, F. Huang, A. I. Cooper, *J. Am. Chem. Soc.* **2017**, *139*, 2908–2911; c) K. Jie, Y. Zhou, E. Li, R. Zhao, M. Liu, F. Huang, *J. Am. Chem. Soc.* **2018**, *140*, 3190–3193; d) K. Jie, M. Liu, Y. Zhou, M. A. Little, A. Pulido, S. Y. Chong, A. Stephenson, A. R. Hughes, F. Sakakibara, T. Ogoshi, F. Blanc, G. M. Day, F. Huang, A. I. Cooper, *J. Am. Chem. Soc.* **2018**, *140*, 6921–6930; e) K. Jie, Y. Zhou, E. Li, R. Zhao, F. Huang, *Angew. Chem. Int. Ed.* **2018**, *57*, 12845–12849; *Angew. Chem.* **2018**, *130*, 13027–13031; f) E. Li, Y. Zhou, R. Zhao, K. Jie, F. Huang, *Angew. Chem. Int. Ed.* **2019**, *58*, 3981–3985; *Angew. Chem.* **2019**, *131*, 4021–4025.
- [34] J. P. Garcia Villaluenga, A. Tabe-Mohammadi, *J. Membr. Sci.* **2000**, *169*, 159–174.
- [35] Crystallographic data for C<sub>6</sub>H<sub>6</sub>@T[5]-(OMe)<sub>5</sub>: C<sub>52</sub>H<sub>50.77</sub>O<sub>5</sub>; colorless block, 0.15 × 0.15 × 0.1 mm<sup>3</sup>; monoclinic, space group P2<sub>1</sub>/c;  $a = 13.07000(10)$ ,  $b = 25.2860(2)$ ;  $c = 13.24560(10)$  Å;  $\alpha = \gamma = 90$ ,  $\beta = 106.9020(10)$ ;  $V = 4188.42(6)$  Å<sup>3</sup>;  $Z = 4$ ;  $\rho_{\text{calc}} = 1.198$  g cm<sup>-3</sup>;  $2\theta_{\text{max}} = 149.61$ ;  $T = 160(10)$  K; 78807 reflections collected, 8439 independent, 550 parameters;  $\mu = 0.595$  mm<sup>-1</sup>;  $RI = 0.0409$  [ $I > 2\sigma(I)$ ],  $wR2 = 0.1006$  (all data).<sup>[37]</sup>
- [36] a) B. Olenyuk, M. D. Levin, J. A. Whiteford, J. E. Shield, P. J. Stang, *J. Am. Chem. Soc.* **1999**, *121*, 10434–10435; b) J. Bacsa, R. J. Less, H. E. Skelton, Z. Soracevic, A. Steiner, T. C. Wilson, P. T. Wood, D. S. Wright, *Angew. Chem. Int. Ed.* **2011**, *50*, 8279–8282; *Angew. Chem.* **2011**, *123*, 8429–8432; c) C. Ren, F. Zhou, B. Qin, R. Ye, S. Shen, H. Su, H. Zeng, *Angew. Chem. Int. Ed.* **2011**, *50*, 10612–10615; *Angew. Chem.* **2011**, *123*, 10800–10803; d) S. Pasquale, S. Sattin, E. C. Escudero-Adán, M. Martínez-Belmonte, J. de Mendoza, *Nat. Commun.* **2012**, *3*, 785; e) D. Fujita, Y. Ueda, S. Sato, H. Yokoyama, N. Mizuno, T. Kumasaka, M. Fujita, *Chem* **2016**, *1*, 91–101; f) Y.-S. Chen, E. Solel, Y.-F. Huang, C.-L. Wang, T.-H. Tu, E. Keinan, Y.-T. Chan, *Nat. Commun.* **2019**, *10*, 3443.
- [37] CCDC 1957868, 1896025, 1957871, and 1957867 (T[5]-(OMe)<sub>5</sub>, CH<sub>3</sub>CNCT[5]-(OMe)<sub>5</sub>, H<sub>2</sub>OCT[5], and C<sub>6</sub>H<sub>6</sub>@T[5]-(OMe)<sub>5</sub>) contains the supplementary crystallographic data for this paper. These data can be obtained free of charge from The Cambridge Crystallographic Data Centre.

Manuscript received: October 12, 2019

Accepted manuscript online: November 25, 2019

Version of record online: January 21, 2020